Creep, Shrinkage and Durability Mechanics of Concrete and other Quasi-Brittle Materials
Edited by F.-J. Ulm, Z.P. Bažant and F.H. Wittmann

Asymptotic temporal and spatial scaling of coupled creep, aging, diffusion and fracture processes

Zdeněk P. Bažant[a] and Daniele Ferretti[b]

[a]W.P. Murphy Professor of Civil Engineering and Materials Science, Department of Civil Engineering, Northwestern University, 2145 Sheridan Road, Evanston, IL 60208.

[b]Visiting Scholar, Northwestern University. [1]

The paper reviews the scaling aspects of various physical mechanisms involved in concrete creep and durability problems. Understanding of these aspects, and especially the asymptotic scaling, is essential for developing realistic materials models valid over a broad range of response times and structure sizes, which are of particular concern for extrapolating from reduced-scale short-time laboratory tests to the full structure sizes and design lifetimes. The scaling aspects are discussed in relation to the coupling of creep with aging, hygro-thermal processes and diffusion processes in concrete. The mathematical structures of the recently developed microprestress-solidification theory of concrete creep and of model B3 are explained by various scaling considerations. The interplay with the spatial scaling of cracking and fracture phenomena is also discussed. The benefit of setting the time scale in shrinkage prediction by means of weight load measurements is pointed out. The mathematical approach to the stresses and early fracturing of a nuclear containment wall due to hydration heat is discussed. Finally, the question as to why many ancient masonry towers either collapse or are endangered after centuries of faultless existence is considered. Based of numerical simulations relevant to the collapse in 1989 of the Civic Tower of Pavia in Italy, it is proposed that the explanation must be sought in the interaction drying times, creep rates and size effect in compression failure.

1. INTRODUCTION

Discovered in 1907 by Hatt [52], the creep of concrete has been researched for almost a century. Enormous progress has been achieved. The theory of linear aging viscoelasticty, which provides the simplest approximation to creep under service conditions, is now so well understood that further research efforts seem unlikely to lead to any major rewards. However, the level of understanding is still quite limited for the coupling of creep with other physical and chemical processes, particularly the aging, hygro-thermal, diffusion and fracturing processes. These couplings, which are very important for the durability of concrete structures, are chosen as the main subject of this lecture.

[1]on leave from Department of Civil Engineering, University of Parma, Parco Area delle Scienze 181/A, 43100 Parma, Italy.

The mathematical modeling of such couplings involves two basic problems: (1) The thermodynamic considerations, which impose various symmetries along with inequalities ensuring non-negativeness of energy dissipation or non-divergence of creep curves, and (2) the asymptotic temporal and spatial scaling in time and space. The present lecture will focus strictly on the latter problem, whose understanding is essential for developing sound mathematical models of broad applicability and for connecting accelerated reduced-scale laboratory tests to engineering applications. To facilitate a clear discussion, the physical mechanisms of creep and shrinkage will also be reviewed to some extent.

A prominent role in durability problems is played by the characteristic times and lengths (sizes), which separate opposite asymptotic trends. In this regard, it is worth keeping in mind the elementary case of a physical process $f(t)$ that involves no characteristic time and, therefore, must be self-similar for short and long times. In analogy to well-known arguments in fluid mechanics [55,5,6,33], we must have in that case [10],

$$f(t_2) \,/\, f(t_1) = f(t_2/t_1) \tag{1}$$

where t_1 and t_2 are any two times. This is a functional equation which is obviously satisfied by a power function, $f(t) = t^n$ (n = constant). It can be proven that a power function is the only solution.

By a similar argument, if a structure possesses no characteristic dimension (size) D, then the structural response must again scale as a power function of D.

The power scaling is of course trivial, but its limitations and the transitions between different asymptotic power laws are not. In fluid mechanics, such questions have been prominent since the beginning of the last century, but in solid mechanics the merit of determining and exploiting asymptotic scaling has become appreciated only recently, beginning with the size effect in quasibrittle failures of concrete structures.

2. MECHANISM OF CREEP AND ITS COUPLING WITH AGING

At variable hygro-thermal conditions, the creep with elastic strain is defined as the strain difference between a loaded specimen and a load-free companion specimen, which undergoes shrinkage and thermal expansion. Drying shrinkage is caused by compressive stresses in the microstructure balancing changes in the capillary tension and surface tension on pore walls as well as the disjoining pressure in hindered adsorbed water layers. The chemical processes of portland cement hydration cause autogeneous shrinkage, which is observed in sealed specimens and amounts to only about 5% of drying shrinkage (but much more in high strength concretes). Creep is caused by slips due to bond ruptures (with restorations at adjacent sites) in the hardened portland cement paste. The paste is strongly hydrophyllic, having a disordered colloidal microstructure, porosity about 0.4 to 0.55, and an enormous internal surface area—about 500 m^2/cm^3; its main component is the tri-calcium silicate hydrate gel ($3\ CaO \cdot 2\ SiO_3 \cdot 3\ H_20$, in short $C_3S_2H_3$); it forms crystalline sheets and needles of colloidal dimensions, weakly bound by van der Waals forces.

At service stresses in structures and in absence of cracking, the creep strain depends on stress linearly. It is commonly characterized by the compliance function $J(t,t')$, defined as the strain ϵ at time (or age) t caused by a unit uniaxial stress σ =1 applied at age t'

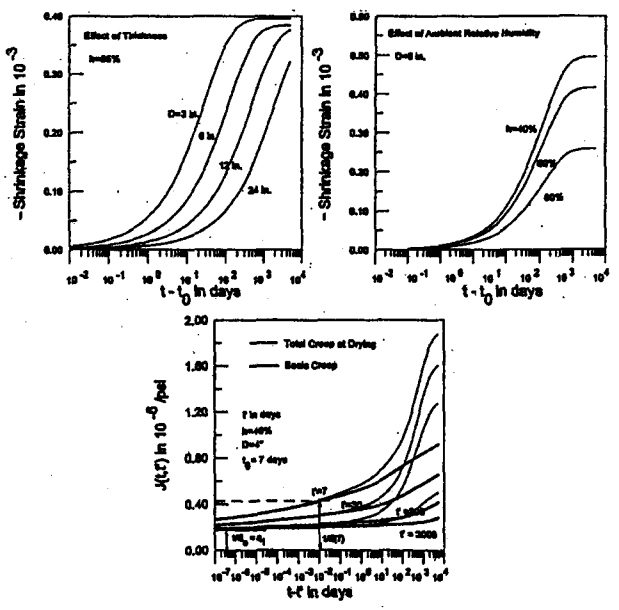

Figure 1. Typical curves of basic creep (left), shrinkage (middle) and creep at drying (right) according to model B3.

(Fig. 1 left). For variable uniaxial stress $\sigma(t)$ as well as triaxial stress, the strain may be obtained according to the Boltzmann-Volterra principle of superposition.

A creep model [25,17] that appears to fit the experimental evidence quite well (and is used in the so-called Model B3 [11,14]) may be conveniently expressed in terms of the compliance rate:

$$\dot{J}(t,t') = v^{-1}(t)\,\dot{C}_g(\theta) + 1/\eta_f \tag{2}$$

$$v^{-1}(t) = q_2\,(\lambda_0/t)^m + q_3 \tag{3}$$

$$\dot{C}_g(\theta) = \frac{n\theta^{n-1}}{\lambda_0^n + \theta^n}, \qquad \theta = t - t' \tag{4}$$

with the initial value of J being an age-independent constant, $J(t,t') = q_1$; $\dot{o} = \partial o/\partial t$; θ=load duration; $\lambda_0 = 1$ day, $m = 0.5$, n= 0.1; q_2, q_3 = dimensionless constants; $C_g(\theta)$ = (age-independent) compliance function for delayed elasticity of the cement gel (hardened cement paste without its pores); $v(t)$ = volume of gel per unit volume of concrete, growing due to hydration; and η_f = effective viscosity for the flow of concrete. Eq. (2) cannot

be integrated analytically to yield a closed-form expression for the compliance function. However, $J(t,t')$ can be easily obtained by numerical integration. For computer structural analysis in short time steps, an expression for $J(t,t')$ is not needed. An expression for the rate $\dot{J}(t,t')$ suffices and in fact allows a simpler algorithm.

For creep of sealed specimens at constant temperature, called the basic creep, the flow term may be written as

$$1/\eta_f = q_4/t \qquad \text{(at constant } w\text{)} \tag{5}$$

where q_4 = dimensionless constant. By integration, the flow part of $J(t,t')$ is simply $q_4\ \ln(t/t')$.

Now let us look at the scaling and asymptotic arguments for the basic structure of these equations. No characteristic time at which the creep evolution would qualitatively change is seen in experiments, and so, in view of Eq. (1), the creep rate should follow a power law (this fact is nicely demonstrated by the logarithmic plots of measured creep rate values presented by Ulm [58]). The power law, however, must get modified by the interference of creep with aging.

Asymptotically, for $\theta \ll t$, there can no appreciable aging during creep, and indeed $\dot{J}(t,t') \approx \theta^{n-1}$ = power curve, according to (4) and (2). As for the opposite asymptotic behavior for $\theta \gg t'$, creep and aging act together, and $\dot{J}(t,t') \approx t^{-1}$, which is again a power curve, but of a different exponent.

The last asymptotic trend is (and must be) also shared by the flow term (5). This trend agrees with the fact that the curves of long-time basic creep are approximately logarithmic functions of time. The transition from the short-time to the long-time asymptotic trend must occur when θ is no longer negligible compared to t, which is roughly when $t \approx 2\theta = 2t'$. This time may therefore be regarded as the characteristic time for the creep curve for a given age at loading t'. Eq. (2) is structured so as to conform to this characteristic time and agree with both opposite asymptotic trends.

Function $C_g(\theta)$ describes the creep of the cement gel, which is a substance whose properties do not vary with age. The aging due to hydration is, according to the solidification theory, caused by the volume growth $v(t)$ of cement gel into the pores in hardened cement paste. Since the rate of hydration is unaffected by load, $\dot{v}(t)$ depends only on time and is also taken as a power function since no characteristic time for volume growth in known (the effect of adiabatic temperature rise, proportional to D^2, is not considered in this argument since it is automatically introduced by taking into account the temperature effect and solving the evolution of temperature distribution).

Eqs. (4), (3) and (5) appear to be the simplest formulae satisfying the aforementioned scaling considerations and asymptotic conditions.

There are other physical arguments leading to power functions for the creep rate, e.g. the activation energy theory [61], but they do not fit the theme of this lecture.

3. MICROPRESTRESS AND COUPLING OF CREEP WITH HYGRO-THERMAL CHANGES

At variable specific water content w (mass of water per unit volume of concrete), a physically realistic constitutive relation may be based on the idea of microprestress S [17],

considered to be a dimensionless measure of the stress peaks whose locations determine the creep sites in the microstructure. The microprestress is considered to be unaffected by the applied load and to be produced solely by chemical volume changes and by changes in the disjoining pressure in the hindered adsorbed water layers (up to ten water molecules, or 2.7 nm, in thickness) confined between sheets of calcium silicate hydrates. Since a local thermodynamic equilibrium, i.e., the equality of the chemical potentials of the hindered adsorbed water and the water vapor in the nearest capillary pores gets established very rapidly (within a fraction of a second), the disjoining pressure, in turn, is a function of temperature T as well as the relative humidity h of the water vapor in the capillary pores. The rate of bond breakages is logically a power function, and particularly a quadratic function, of the level of microprestress. This leads to the expression

$$1/\eta_f = q_4 S \tag{6}$$

which replaces the simple age dependence of η_f applicable for the case of constant hygro-thermal state (constant w and T, sealed specimens). The microprestress relaxes in time and its evolution at each point of a concrete structure may be solved from the differential equation

$$\dot{S} + c_0 S^2 = c_1 \left| \dot{T} \ln h + T \dot{h}/h \right| \tag{7}$$

where c_0, c_1 = positive constants. The absolute value is introduced to ensure that S could never be negative and to reflect the experimental observation that not only drying and cooling but also wetting and heating accelerate creep. A switch from heating to cooling, or drying to wetting, or vice versa, would of course deactivate the current creep sites but it is reasonable to expect that it would activate other creep sites at different locations. The fact that changes of w or h produce new microprestress peaks and thus activate new creep sites explains the drying creep effect (called also the Pickett effect). A part of this effect, however, is caused by the fact that microcracking in a companion load-free specimen makes its overall shrinkage less than the shrinkage in an uncracked (compressed) specimen, thus increasing the difference between the two (which defines creep).

The concept of microprestress is also needed to explain the stiffening due to aging. One physical cause of aging is that the hydration products gradually fill the pores of hardened cement paste, as reflected in function $v(t)$ in (3). But hydration ceases after about one year, yet the effect of age at loading t' is strong even after many years (experiments show a very large creep difference between specimens loaded at 1 year and 7 years of age). The explanation is that the peak microstress gradually relaxes with time, which reduces the number of creep sites and also the rate of bond breakages at these sites.

The fact that the relaxation rate of microprestress S must depend on S is obvious. But why should it be proportional to a power function of S, and particularly a quadratic function, as written in (7)? The explanation is provided again by asymptotic scaling considerations. A power function is logical because the long-term aging shows no distinct characteristic time, and because it affects similarly the creep curves at different applied stress levels. To get a clue about the exponent of the power function, consider the asymptotic case of constant hygro-thermal state ($\dot{h} = \dot{T} = 0$, sealed specimens, basic creep); in that case

$$\dot{S} = -c_0 S^2 \tag{8}$$

the integration of which gives $S = S_0(t_0/t)$ where t = time, t_0 initial time, and S_0 = initial value of S at time t_0. This represents microprestress relaxation that causes the strain in the flow element to grow exactly as a logarithmic function of time, which is necessary for matching long-term creep tests. It is because of this empirical fact that the power function of S in (7) and (8) cannot be other than quadratic.

In the opposite asymptotic case of $\dot{h} \to \infty$, (7) reduces to

$$\dot{S} = -c_1 \frac{\dot{h}}{h} \tag{9}$$

which implies $S = -c_1 \ln h +$ const. This property of Eq. (7) means that, if the change of pore humidity h is very fast, the microprestress varies solely as a function of h. The same holds true for a very fast change of temperature.

In (7), we have a microprestress relaxation law, which replaces the age-dependence of viscosity. The long-term aging of flow viscosity is simply a consequence of relaxation of the microprestress.

At variable environment, time t in (3) must of course be replaced by the equivalent hydration time,

$$t_e = \int \beta_h \beta_T \mathrm{d}t \tag{10}$$

where β_h = decreasing function of h (0 if $h <$ about 0.85) and $\beta_h \propto \mathrm{e}^{-Q_h T/R}$, $Q_h/R \approx$ 2700 K. In (4), $\theta = t - t'$ must be replaced by $t_r - t'_r$ where

$$t_r = \int \psi_h \psi_T \mathrm{d}t \tag{11}$$

is the reduced time, capturing the direct effect of h and T on creep viscosity; ψ_h = function of h decreasing from 1 at $h = 1$ to about 0.1 at $h = 0$; $\psi_T \propto \mathrm{e}^{-Q_v T/R}$, $Q_v/R \approx 5000$ K.

The evolution of distributions $h(\mathbf{x}, t)$ ($\mathbf{x}$ = coordinate vector) may be considered uncoupled from the stress and deformation problem (except when large cracks, wider than about 0.5 mm develop). This evolution may be solved numerically from the diffusion equation whose simplified form is $\dot{h} = \mathrm{div}[C(h)\mathrm{grad}\, h] + \dot{h}_s(t_e)$ where $h_s(t_e)$ = function defining the selfdesiccation caused by hydration (which is mild in normal concretes but strong in high strength concretes), $C(h)$ = diffusivity, which decreases about 20 times as h drops from 100% to 60%. As data fitting with finite element programs confirms, the free (unrestrained) shrinkage strain rates may be very simply expressed as

$$\dot{\varepsilon}_{sh} = k_{sh} \dot{h} \tag{12}$$

where k_{sh} = shrinkage coefficient. Since the values of $\dot{\varepsilon}_{sh}$ at various points of the structure are in general incompatible, the calculation of the overall shrinkage of test specimens as well as structures is a stress analysis problem, in which creep and cracking must be taken into account.

For the purpose of introducing the effect of variable temperature (as well as for the purpose of finite element analysis), it is advantageous to convert the constitutive law to a rate-type form [7,52]. This may be achieved by approximating $C_g(\theta)$ with a Kelvin chain model (or the associated relaxation function with a Maxwell chain model). The history

integrals can then be eliminated from the constitutive law, the history being characterized by the current values of the internal state variables (the partial strains or stresses of the Maxwell or Kelvin chain). The temperature effect on creep rate [19] may be captured by an Arrhenius-type dependence of the viscosities of the units of the Kelvin (or Maxwell) chain. This is, however, only one effect of temperature, an effect in which a temperature rise increases the creep rate. There is another, opposite, effect of temperature on creep, arising from the temperature dependence of the rate of hydration, as captured by t_e. This dependence causes that a temperature rise accelerates the aging process due to hydration, which in turn reduces the creep rate. The former effect usually prevails but in very young concrete not always.

To sum up, the form of the equations of the microprestress constitutive theory of concrete creep is again largely motivated by asymptotic scaling considerations.

4. SCALING OF CREEP-DIFFUSION COUPLING

Drying and wetting of concrete structure strongly influences creep, and if creep and shrinkage produce significant cracking or fracture, then they influence the rate of drying or wetting (or other deterioration processes, e.g. [59,49,32,29]). Before discussing the asymptotic scaling considerations, let us summarize a simplified mathematical model capturing the essential features of the average creep and shrinkage in drying cross sections of concrete structures [11,14].

The average cross-sectional compliance function $\bar{J}(t,t',t_0)$ (Fig. 1 right, light lines) and average shrinkage function $\bar{\varepsilon}_{sh}(t,t_0)$ of the cross section (Fig. 1 middle) where t_0 = age at start of drying, were derived under strong simplifications [11,14] from the foregoing constitutive relations, and their coefficients were optimized by fitting a very large test data bank;

$$\bar{\varepsilon}_{sh}(t,t_0) = -\epsilon_{sh\infty}\, k_h\, S(t), \quad k_h = 1 - h_e{}^3 \tag{13}$$

$$S(t) = \tanh\sqrt{\frac{t-t_0}{\tau_{sh}}}, \quad \tau_{sh} = k_t(k_s D)^2 \tag{14}$$

for environmental humidities $h_e \leq 98\%$; here $D = 2v/s$ = effective thickness, v/s = volume-to-surface ratio, $k_t = 1$ for normal (type I) cement; k_s = shape factor (e.g., 1.0 for a slab, 1.15 for a cylinder); and $\epsilon_{sh\infty} \approx \epsilon_{s\infty}E(607)/(E(t_0+\tau_{sh})$, $\epsilon_{s\infty}$ = constant; $E(t) \approx E(28)\sqrt{4+0.85t}$= age dependence of Young's modulus (all times are in days). Eqs. (2), (3) and (4) apply except that $1/\eta_f$ must now be replaced by

$$\frac{1}{\bar{\eta}_f} = \frac{q_4}{t} + q_5\frac{\partial}{\partial t}\sqrt{F(t)-F(t'_0)} \tag{15}$$

where $F(t) = \exp\{-8[1-(1-h_e)S(t)]\}$ and $t'_0 = \max(t', t_0)$.

The basic structure of these formulae has been derived from a number of asymptotic scaling considerations. The form of the expression for shrinkage halftime τ_{sh} is based on the diffusion theory. The drying and wetting of concrete constitute a nonlinear diffusion problem, and for both linear and nonlinear diffusion the halftime of drying or wetting at constant environment, τ_{sh}, is generally proportional to the square of the characteristic dimension D^2, as written in (14) (deviations of course occur, because of aging and cracking;

but it would be incorrect to think that they change the power of D to other than 2; rather they have different influencing factors, and should they be taken into account, additional functions would need to be introduced into the formulation).

The diffusion theory also indicates that the effect of the shape of cross section, as well as the value of environmental humidity h_e, should enter Eqs. (13) and (14) as multiplicative factors, which means that these influences cause vertical scaling of the drying and shrinkage curves. On the other hand, the effect of size D is manifested, according to (14), as a horizontal scaling of the drying and shrinkage curves as functions of $t-t_0$, which amounts to a horizontal shift by distance $\ln D$ when these curves are plotted as functions of $\ln(t-t_0)$.

Function 'tanh' used in (13) is the simplest one satisfying two asymptotic conditions ensuing from the diffusion theory: (1) for short times, $\bar{\varepsilon}_{sh} \propto \sqrt{t-t_0}$, and (2) the final shrinkage value must be approached exponentially. So the 'tanh' function can be regarded as an asymptotic matching approximation. The former asymptotic property is supported by test data quite well, but the latter only weakly, because test data pertinent to sufficiently long durations are very rare.

Discussing formulae (13)–(15), one cannot miss emphasizing that they are only crude approximations because they ignore the differences due to cross section geometry, reinforcement, cracking extent and distribution, and the type of loading (e.g., differences in the average creep of cross section among loadings by compressive or tensile axial forces, bending moments, shear forces, torques, etc.) To achieve trouble-free designs, the practice should move away from one-dimensional beam-type calculations and toward numerical predictions in which the cross section is subdivided into a number of finite elements. This approach is nowadays quite feasible.

5. IDENTIFYING THE TIME SCALE IN SHRINKAGE PREDICTION BY MEANS OF WEIGHT MEASUREMENTS

It might seem that long time drying shrinkage of a specimen can be predicted by fitting some shrinkage formula such as (14) to short-time measurements. It turns out, however, that this is an ill-conditioned problem, i.e., a problem in which a very small change in the data causes an enormous change in long-time prediction. It was shown [11,14] that the cause of this problem is the uncertainty about the value of the shrinkage half-time τ_{sh}, which sets the time scale of shrinkage process.

The basic idea is to identify τ_{sh} from the measurements of weight loss during the short-time drying shrinkage tests. The difference between the drying shrinkage and the loss of water is that while the final asymptotic value of shrinkage is unknown, the final asymptotic value of weight loss can be closely estimated in advance. This can be done in two ways: by measuring the weight loss caused by oven heating at the end of short-time test, or by calculations based on the amount of water in the concrete mix. Once the final weight loss in known, τ_{sh} can be easily evaluated.

6. SIZE EFFECTS DUE TO CRACKING AND DISTINCT FRACTURES

By far the most frequent undesirable consequence of misprediction of creep and shrinkage is the cracking (or fracture), which often triggers various chemical deterioration pro-

cesses reducing durability of the structure. In the simplest approximation, the coupling of creep and shrinkage with fracture is considered to go one way, fracture being the consequence. However, the cracking, in reverse, also affects the creep of structures, and does so in various ways. The reverse effects of cracking on creep are mainly two: (1) The distributed cracking (modeled as nonlocal strain softening) or fracture causes a redistribution of stresses in the structure, which of course alters the subsequent evolution of creep. (2) The cracks may serve as significant conduits for the exit of moisture, i.e., the drying process may get accelerated, which then intensifies both shrinkage and drying creep. The latter effect, though, is significant only for cracks wider than about 0.5 mm [28].

A number of asymptotic scaling considerations arise in the interaction of creep and shrinkage with fracture [51]. One is the size effect on nominal strength of structures with propagating large fractures and cracking zones. This subject has recently been discussed at great depth.

Another, quite important but usually ignored, effect is the crack opening width. For a given overall strain, the width of cracks is proportional to the average crack spacing. The spacing depends on many factors and its determination is in fact a problem of stability and bifurcation in the evolution of a crack system.

7. COUPLING OF CREEP WITH THERMAL AND FRACTURE EFFECTS

As an example of interaction with thermal and fracturing effects, this section will discuss the hydration heat effects in a nuclear containment wall. The exposition of this section will closely follow a previous report [8].

The characteristic times of heating or drying of a concrete wall of thickness H may be defined as the times needed for the heating or drying fronts propagating from the opposite heated faces of the wall to meet at mid-thickness. They are expressed as

$$\tau_{ch}^{T} = H^2 \,/\, 12\,\kappa_T, \qquad \tau_{ch}^{w} = H^2 \,/\, 12\,\kappa_w \tag{16}$$

where H = wall thickness and κ_T, κ_w = diffusivities of heat and moisture in concrete. The typical values of the diffusivities of concrete are $\kappa_T = 0.4$ cm^2/s and $\kappa_w = 0.1$ cm^2/ day (for mature concrete). Thus the typical characteristic times are $\tau_{ch}^{T} = 4.5$ years and $\tau_{ch}^{w} =$ 27 min. The times needed for an almost uniform temperature or humidity across the wall are about 50-times longer, i.e., about 22.5 days and 22.5 years, respectively. From these time scales it is clear that, for example, moisture diffusion can be neglected in estimating the overall hydration heat effects on the wall, the duration of which is of the order of weeks.

The evolution of temperature profiles is governed by the heat conduction equation with a source term depending on temperature and the current equivalent age (maturity) of concrete. The heat conduction may be assumed independent of the deformations and cracking of concrete. Numerical solution by finite differences is easy and may be carried out according to the well-known Crank-Nicolson algorithm [37].

We assume that during the heating of concrete by hydration, the resultant forces in the cross section of a wall (per unit length of the wall) include only the normal force N_y, which is given, while the bending moments $M_y = M_z = 0$. For the sake of simplicity, we

also assume that the normal forces in the y and z directions are the same, $N_z = N_y$. The in-plane normal strain ϵ in the wall is uniform throughout the wall thickness h and is the same in both directions, $\epsilon_y = \epsilon_z = \epsilon$. The in-plane normal stresses σ are also the same in both directions but vary throughout the thickness.

The heating is likely to produce parallel equidistant thermal cracks emanating from both faces of the wall, some normal to the axis y and others normal to axis z. As usual, they are assumed in calculations to be continuously smeared. This means that, despite crack formation, each cross section of a long wall may be considered to be in the same state and remain planar, and that $\sigma_{xy} = \sigma_{xz} = \sigma_{yz} = \sigma_x = 0$.

The solution of stresses in presence of temperature and age-dependent creep is coupled with cracking. To take cracking and fracture into account in a simple manner, one may use the crack band model ([21], which approximately takes into account the localization of distributed cracking into discrete cracks. These cracks tend to have a certain characteristic spacing s. Because the adjacent crack bands cannot overlap, the minimum possible spacing of these cracks must be taken equal to the empirically known width w_c of the crack band (or the fracture process zone); w_c must be considered to be a material property (in order to avoid false localization and spurious mesh sensitivity, and to ensure correct energy dissipation); roughly $w_c \approx 3d_a$ where d_a = maximum aggregate size.

When the parallel thermal cracks get too long compared to their spacing, every other crack closes and the spacing of the remaining (dominant) cracks increases. Based on the analysis of equilibrium path bifurcation in a system of parallel thermal cracks [22,23,15], it was shown [27] that the spacing of the dominant (open) cracks increases roughly as

$$s = 0.69\,a \tag{17}$$

where a = length of the cracks (Fig. 2). In view of the crack band model restriction on the crack band width and the corresponding minimum spacing, the general rule for the dominant crack spacing may be approximately written as

$$s = \mathrm{Max}(\,3d_a,\, 0.69\,a) \tag{18}$$

Let ξ be the accumulated cracking (or fracturing) normal strains in the y and z directions. The strain in the concrete between the cracks is $\epsilon - \xi$. Therefore, applying the principle of superposition for creep of concrete [7,52], the biaxial creep law with aging and cracking may be written in the form [16]:

$$\epsilon(t) - \xi(t) = \int_0^t J(t,t')\sigma(x,\mathrm{d}t') + \alpha[T(x,t) - T_0] \tag{19}$$

Here $t = 0$ corresponds to the instant of the set of concrete (i.e. the moment the concrete ceases to be a liquid); α = thermal expansion coefficient of concrete (about 10^{-5}); $\sigma(x,\mathrm{d}t') = [\partial\sigma(x,t')/\partial t']\mathrm{d}t'$ if s varies continuously; $J(t,t') = (1-\nu)J_1(t,t')$ = now denotes the biaxial compliance function of concrete while $J_1(t,t')$ now represents the uniaxial compliance function; and ν = Poisson ratio of concrete ($\nu \approx$ constant $= 0.18$).

Assuming symmetric stress profiles in the wall, the strain ϵ may be considered to be constant throughout the wall thickness. For a numerical solution, one subdivides x by nodal n points $x_i (i = 1, 2, ...n)$ into $n-1$ equal steps Δx, and time t by discrete times $t_r (r = 1, 2, ...N)$ into time steps $\Delta t = t_{r+1} - t_r$, which may be increased with time.

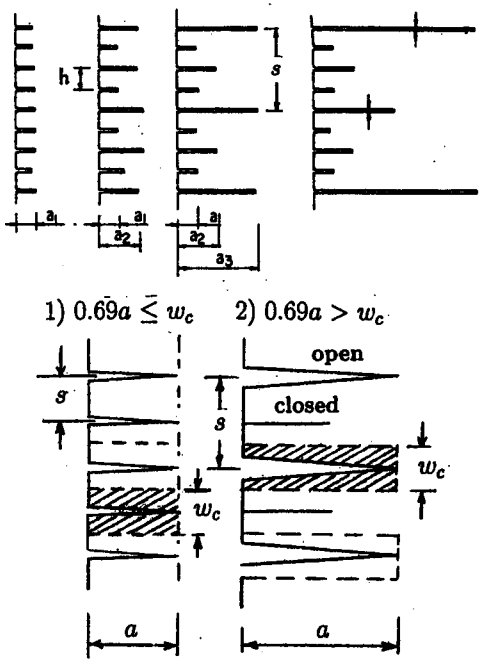

Figure 2. Top: Evolution of a system of parallel thermal cracks and crack spacing as a function of crack length (after Bažant et al. 1979). Bottom: Crack system limited by minimum spacing w_c equal to width of crack band (fracture process zone).

Differentiating (19) with respect to t and multiplying by time increment $\Delta t = t_{r+1} - t_r$, we obtain for the strain increment $\Delta\epsilon = \epsilon_{r+1} - \epsilon_r$ the following central difference approximation:

$$\Delta\epsilon = J_{r+\frac{1}{2},r+\frac{1}{2}}\Delta\sigma_i + \Delta t\sum_{q=1}^{r-1} J_{r+1,q+\frac{1}{2}}(\sigma_{i,q+1} - \sigma_{i,q}) + \alpha\Delta T_i + \Delta\xi_i \tag{20}$$

with the short notation $J_{r,q} = J(t_r, t_q)$; subscript $r + \frac{1}{2}$ refers to time $(t_r + t_{r+1})/2$.

Equilibrium in the cross section requires that $\int_0^h \sigma(x,t)\mathrm{d}x = N_y(t)$ or, in discrete form,

$$\sum_{i=1}^{n} c_i\sigma_{i,r} = N_{y_r} \qquad (r = 1, 2, ...N) \tag{21}$$

where $\sigma_{i,r}$ = stress value at node i at time t_r, and c_i are the coefficients of trapezoidal numerical integration formula ($c_1 = c_n = \Delta x/2, c_2 = ... = c_{n-1} = \Delta x$).

According to the crack band model or the cohesive crack model, the crack-bridging (cohesive) stress as a decreasing function of the accumulated cracking strain ξ may be characterized as:

$$\xi = \psi(\sigma) \qquad (\xi \geq 0) \tag{22}$$

(Fig. 3). This function may be taken as the inverse of the function

$$F(\xi) = f(\delta) = f(\, s\xi\,) \tag{23}$$

where $s\xi = \delta$ = opening width of the actual cracks, s = spacing of these cracks (Fig. 2), and $f(\delta)$ = softening function used in the cohesive (or fictitious) crack model [24]. This function may be taken as a bilinear, starting at $\sigma = f_t'$ for $\delta = \xi = 0$ and terminating at $\sigma = 0$ for some critical opening δ_f.

Because of creep, Irwin's characteristic length of fracture, $l_{ch} = E'G_f/f_t'^2$ (with E' = effective elastic modulus for plane stress or strain) is not a constant because, in the case of creep, E' must be replaced by the effective modulus for creep $E_{ef} = E'/(1+\varphi)$ where φ = creep coefficient. This means that the spatial scaling of fracture gets modified by creep, as indicated by the age-dependence of the characteristic length [9]:

$$l_{ch}(t', t) = \frac{E'G_f}{[1 + \varphi(t', t)]f_t'^2} \tag{24}$$

The consequence of this scaling is that the fracture process zone is getting shorter, the response more brittle, and the size effect stronger, as the load duration increases (this is relevant to the example of ancient tower collapse discussed later).

The thermal stresses caused by hydration heat are compressive in the core and tensile near the surfaces. The main concern is the cracking that may be caused by the tensile stresses. The increment of cracking strain at node i may be written as

$$\Delta\xi_i = C\Delta\sigma_i \tag{25}$$

where C = tangential compliance of cracking, which depends on other variables. Equation (20) may now be rewritten in the quasielastic form

$$\Delta\epsilon = (C_v + C_i)\Delta\sigma_i + \Delta\epsilon_i^v + \alpha\Delta T_i + C_i\Delta\sigma_i \tag{26}$$

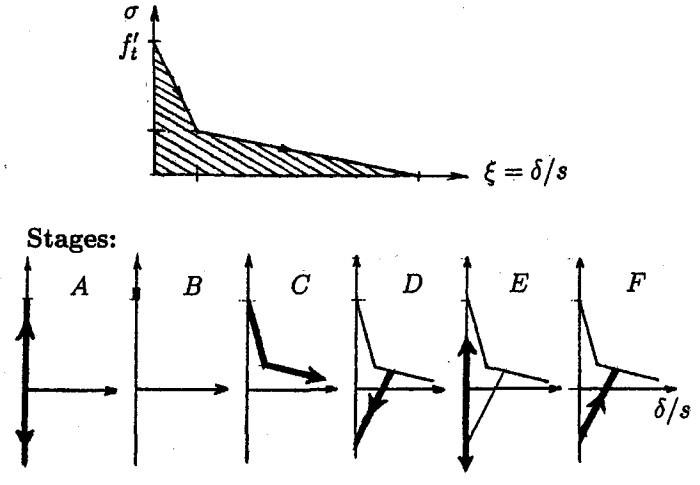

Figure 3. Top: Tensile stress-strain relation of cracked concrete based on the cohesive crack model. Bottom: Stages of loading, unloading and reloading.

in which

$$C_v = [J_{r+1,r+1} + J_{r,r} + \Delta t(\dot{J}_{r+1,r} + \dot{J}_{r+1,r+1})]/2 \tag{27}$$

$$\Delta\epsilon_i^v = \sum_{q=1}^{r-1} \Delta t/2(\dot{J}_{r+1,r} + \dot{J}_{r+1,r+1})(\sigma_{i,q+1} - \sigma_{i,q}) \tag{28}$$

C_v = effective incremental compliance and $\Delta\epsilon_i^v$ = effective inelastic strain increment due to viscoelasticity (creep). Both these quantities can be evaluated before solving the variables for t_{r+1}.

The step-by-step solution of stresses and strains may proceed in time step (t_r, t_{r+1}) according to the following algorithm.

1. Loop over all nodes $i = 1, ...n$
2. Evaluate C_v and $\Delta\epsilon_i^v$ from (27) and (28). Set $I = 1$ (first iteration)
3. For the first iteration, $I = 1$, and for all nodes $i = 1, ...n$, estimate the average and final stress values in the step as $\bar{\sigma}_i = \sigma_{i,r}$.
4. Loop on iterations, $I = 1, ...N_{it}$
5. If $\xi_i > 0$, go to 10.
6. Now we have $\xi \leq 0$ (stage A, B or E, Fig. 3). Set $C_i = 0$.
7. If $\bar{\sigma}_i < f_t'$ (stage A or E), go to 15.
8. Now we have $\bar{\sigma}_i \geq f_t'$ (stage B). Set $C_i = \psi'(\bar{\sigma}_i)$.
9. Go to 15.
10. If $\Delta\xi_i \leq 0$ (crack unloading, stage D), go to 14.
11. Now we have $\xi_i > 0$ and $\Delta\xi_i > 0$. If $\bar{\sigma}_i < \psi(\bar{\sigma}_i)$, go to 13.
12. Virgin crack loading (stage C). Set $C_i = \psi'(\bar{\sigma}_i)$ and go to 15.
13. Reloading of crack (stage F). Set $C_i = C_u$ and go to 15.
14. Unloading of crack (stage D). Set $C_i = C_u$.
15. End of the loop on nodes $i = 1, ...n$.
16. According to equilibrium condition (21), calculate

$$\Delta\epsilon = \left[\sum_{i=1}^{n} \frac{C_i}{C_v + C_i}(\Delta\epsilon_i^v + \alpha\Delta T_i) + \Delta N_{y_{i,r+1}} - \Delta N_{y_{i,r}}\right] \Big/ \sum_{i=1}^{n} \frac{C_i}{C_v + C_i} \tag{29}$$

17. For all nodes, $i = 1, ...n$, calculate

$$\Delta\sigma_i = \frac{\Delta\epsilon - \Delta\epsilon_i^v - \alpha\Delta T_i - C_i\Delta\sigma_i}{C_v + C_i} \tag{30}$$

and set $\bar{\sigma}_i = \sigma_{i,r} + (\Delta\sigma_i/2)$, $\hat{\sigma}_i = \sigma_{i,r} + \Delta\sigma_i$.

18. If $I < N_{it}$ (end of iteration loop), reset $I \leftarrow I + 1$ and go to 5.
19. Start the next time step. Reset $r \leftarrow r + 1$ and go to 1.

While, in the foregoing simple example, the creep analysis is based on the compliance function, more complex problems require the formulation to be based on the Kelvin or Maxwell chain model.

Eq. (18) is an essential scaling property of the problems of thermal or drying cracks. Its effect is to destroy similarity of stress distributions and cracking in thin and thick walls ([27]). It causes the the effective strain-softening due to thermal stresses in thick walls is steeper than in thin wall. Especially, this scaling property must not be neglected in extrapolations from reduced-scale short-time laboratory tests to real structures.

8. SPACE-TIME INTERACTION MAPS

The typical time curve of heat content or water content of a specimen exposed to constant environment different from that within the pores of concrete has the approximate sine-hyperbolic shape that has already been mentioned and is shown in Fig. 1. Such an evolution applies to many other variables occurring in concrete durability problems. In these problems, many orders of magnitude of response duration need to be considered when reduced-scale short-time tests need to be extrapolated to real structures.

Most of the transition from the initial value to the final asymptotic value typically occurs within one order of magnitude of time, and virtually all of it within two orders of magnitude. Therefore, in relations to response time scale spanning many orders of magnitude, the transition may considered to occur suddenly, at a time equal to the halftime of the process, e.g., τ_{sh}. Thus the response may approximately be described as Heaviside function of time, having a step at $t = \tau_{sh}$, i.e., as $H(t - \tau_{sh})$ or $H(t/\tau_{sh})$.

In an infinite halfspace, the distance x of the front of heating or drying or any other diffusion-type process from the surface increases as $x = \sqrt{12\kappa t}$ where κ = material diffusivity. The rule applies asymptotically for short times even if the body is finite, and may be used as a rough approximation until the time the fronts propagating from the opposite faces of a wall meet.

Using the foregoing approximations, one can sketch simple space-time interaction maps such as that for a drying wall shown in Fig. 4), in which thin and thick walls are compared. In the sense of the Heaviside function approximation, the saturated ('wet') states in a drying wall are represented by the shaded wedge-shaped domain in the figure, and the dried states by the rest of domain. The boundary between the domains is straight because the coordinate is chosen as $\sqrt{t}$ rather than t. The corresponding evolutions of the average shrinkage of the wall in $\sqrt{t}$ are plotted beneath, and further beneath the evolutions of the maximum shrinkage stress within the wall as affected by creep and by the humidity effect on creep. The effect of creep is small in thin walls but can be quite large in thick walls which take far longer to dry out. While generally creep causes stress relaxation, the nonuniformity of creep within the cross section (due to differences in moisture states) may cause the maximum stress in the cross section to increase.

9. HOW SCALE EFFECTS IN DIFFUSION, CREEP AND FRACTURE CAN CONSPIRE TO ENDANGER ANCIENT TOWERS AFTER ABOUT 10^3 YEARS

Coupled temporal and spatial scale effects are very important in durability problems. Let us now look at one example where these effects conspire to endanger structural stability after a very respectable lifetime of unperturbed existence for about 10^3 years.

In 1989, seven centuries since its construction, the Civic Tower of Pavia (Fig. 5a) in Italy collapsed suddenly, with imperceptible warning signals. This dramatic event was only the last in a series of failures masonry towers of the height of 60 m or more, built in Italy between 11th and 14th century [44]. One was the 1902 collapse of the Bell Tower in San Marco Square in Venice [45]. The famous tower in Pisa is not only leaning but its masonry endangered [46,48].

The walls of these towers usually consist of two external layers (claddings) of good

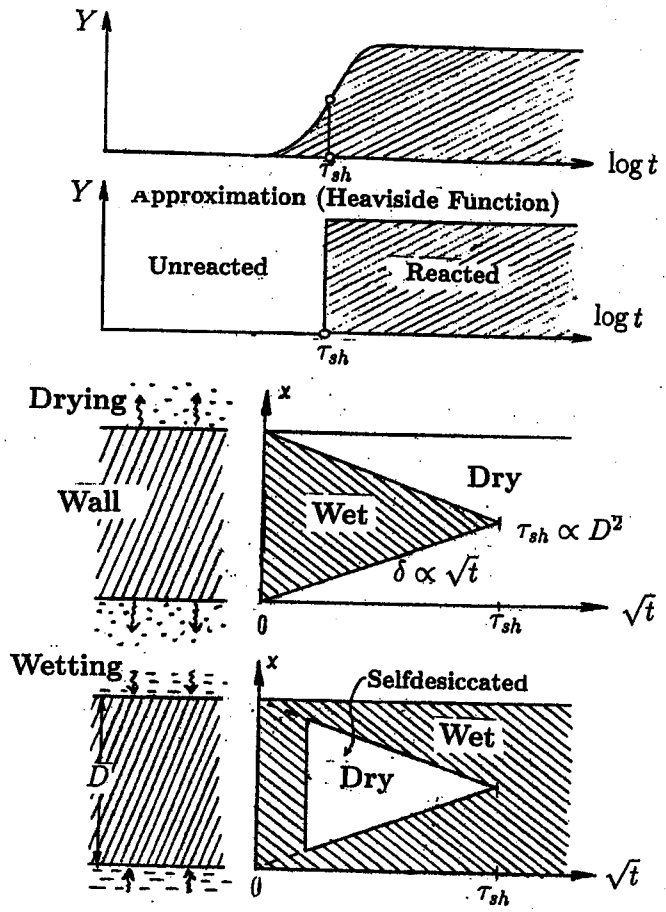

Figure 4. Top: Typical evolution of reaction degree Y over many orders of magnitude of time t and its approximationa by Heaviside step function. Bottom: Interaction of temporal and spatial scales in the problems of drying of a wall, and wetting of a wall with selfdesiccation.

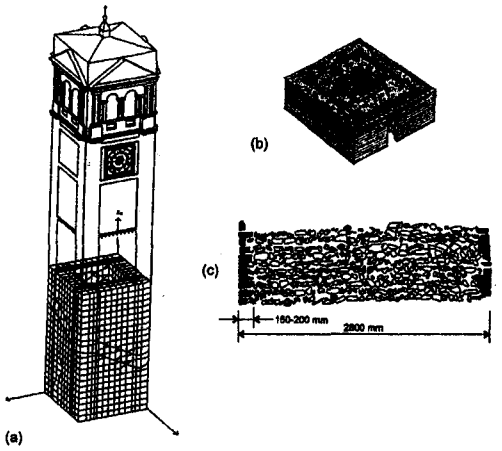

Figure 5. Civic Tower of Pavia - Italy [34]: (a) geometry and finite element mesh; (b) generic cross section; (c) masonry wall.

coursed masonry 150–250 mm thick, filled up by about 2 m (generally 1–3 m) of a particular ancient concrete consisting of lime mortar, river gravel and recycled bricks (Fig. 5). Fissures in these walls and the tendency of the external layers to spall off was discussed by Jamiolkowski et al. [46].

After many centuries of uneventful existence, several damaged or collapsed towers were seen to develop a significant growing crack patterns attributable to vertical compression, with a network of superficial vertical microcracks propagating through mortar joint and also cutting through the bricks. In most of these cases, foundation settlements, overloads and chemically induced decay were excluded as the cause of cracking. The average stresses due to the weight of these towers are generally modest. For instance, in the case of the Civic Tower of Pavia, the average vertical normal stress was only 1.1 MPa while the uniaxial compressive strength was measured to be about 2.8 MPa [36,34]. Notwithstanding, the the three-dimensional nonlinear finite element analyses that have been conducted [36,34] showed that a severe stress concentration exhausting the compression strength existed at the base of the stairwell, near the entrance. However, although it must have triggered local failure, as confirmed by the ruins, neither the overall collapse nor the development of crack patterns prior to collapse could be explained by these finite element analyses. Obviously, the problem was that these sophisticated numerical simulations have not taken into account the effect of time.

Time effects are certain to arise from creep and drying of the wall. Creep of the specimens of the ancient concrete taken from the ruins of the Pavia tower was measured by

Anzani et al. [3,4] and found to be quite pronounced (Fig. 6). In highly compressed specimens, the researchers also noticed progressive growth of splitting microcracks and were able to distinguish primary, secondary and tertiary creep. They suggested that development of localized high compression stresses, together with fatigue under cyclic wind and temperature stresses, led to tertiary creep and thereby to collapse. The hypothesis of non-uniform distribution of stresses across the walls was in effect confirmed by measuring the stresses in some towers by means of flat-jacks, e.g. [38]. This nonuniformity could be related not only to geometric stress concentrators (e.g. corners, stairwell, windows, and tilting) but also to creep behavior similar to that observed in young masonry walls [47]. An analogy could be drawn with the case of modern multi-layer walls where the effects of moisture diffusion, drying and creep are known to cause microcracks due to redistribution of stresses among different layers [1].

The walls of ancient towers must be expected to exhibit not only creep but also drying shrinkage and drying creep, similar to modern concretes. The cladding consisting of marble, stone or brick masonry creeps and shrinks very little. Shrinkage of the lime concrete core must eventually cause high compressive stresses in the cladding. Creep (basic creep as well as drying creep) of the core must further cause gradual transfer of stresses from the core to the cladding. Why should this process take 700 years?

The temporal scale is set by the diffusion of moisture through the massive concrete wall, and is somewhat modified by creep. Assuming the ancient concrete to have roughly the same diffusion properties as a modern low-strength concrete, the time for the wall to dry up is just about 700 years.

During the initial stage of drying, concrete near the exterior cladding shrinks and additionally contracts due to drying creep. This causes it to develop additional tensile stresses, which must be balanced by stress increase in the central portion of the wall and in the cladding. The stresses in concrete, though not those in the cladding, relax due to creep. During the terminal stage of drying, the central portion of the wall shrinks and additionally contracts due to drying creep. This reduces compressive stresses in the central portion, which must be balanced by an increase of compressive stresses both in the cladding and in the concrete near the cladding. The increase of compressive stress may cause compression failure of the surface layer of the wall, which can take the form of either crushing of the masonry with the adjacent concrete, or delamination buckling of the cladding.

In either case, the compression failure may be expected to involve a transverse propagation of a failed layer in which the masonry is in the postpeak softening range of its stress-strain diagram. The compression stresses in the failed layer are reduced, which causes unloading of the adjacent zones of the cladding and the core.

Here the spatial scale intervenes again. The unloading of the zones adjacent to the failed layer implies a release of strain energy, which must get dissipated somewhere. It gets dissipated by flowing into the front of the failed layer and driving its propagation. Owing to the large dimensions of the wall, the result must be a size effect—i.e., the apparent, or nominal, strength of the masonry cladding must be less than that measured on laboratory specimens [39,40]. The length of the failed layer at collapse may reasonably be assumed to be proportional to the cross section dimension of the wall. The cause of the size effect is the fact that the volume of the partially unloaded zone on the flanks of

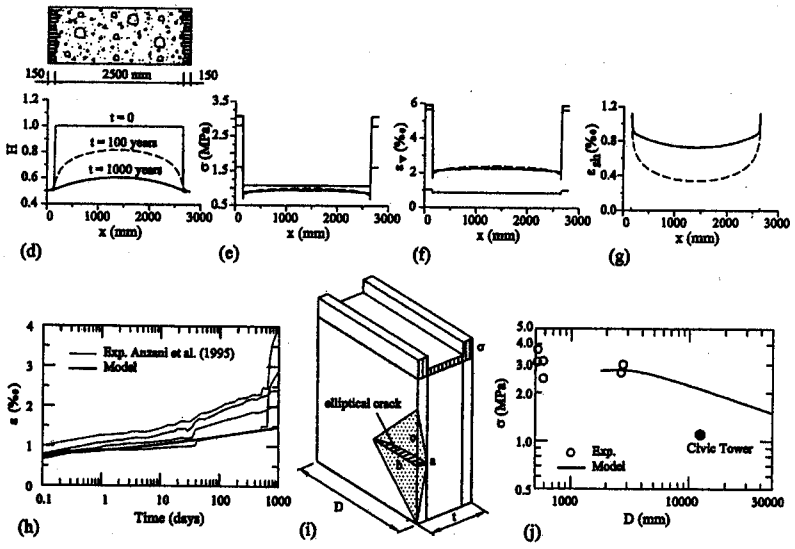

Figure 6. Pavia tower analysis: (d-g) Evolution of distributions of shrinkage stress, creep strain and shrinkage strain. (h) Creep measured on ancient masonry specimens (after [3]). (i) Three-dimensional model of wall with cladding under nonuniform stress, and assumed failure mode. (j) Size effect of as a function of tower size.

the failed layer, and thus also the energy released from that zone, grow quadratically with the length of the failed layer, while the energy consumed by fracturing at the front of the failed layer grows linearly. Obviously, energy could not be in balance if the stresses before failure were the same for long as well short failed layers.

To demonstrate the possibility of the proposed scenario just outlined, the diffusion, shrinkage, creep, evolution of stress distributions, and the propagation of the failure of the excessively compressed cladding are simulated numerically. Fig. 6 presents some of the numerical results, while a detailed presentation is planned for a journal article in preparation.

Fig. 6d shows the calculated distributions of pore relative humidity across the wall at the ages of 100 years and 1000 years. Fig. 6e shows the distributions of vertical compressive stresses at the basis of the tower, due own weight. At time $t = 0$, cladding sustains heavier stresses, owing to higher stiffness of bricks. During time, an enormous transfer of compressive stress into the cladding should be noted. After centuries the stress in the cladding roughly reaches the strength measured in laboratory tests [36,34].

Fig. 6f shows the distributions of creep strains ϵ_V in the lime concrete (the reason that, at time $t = 0$, the distribution is not uniform is that the mortar joints in the cladding are more stressed). As already pointed out, the shape of the strain profile varies during time, due to the interaction with shrinkage strain. Fig. 6g represents the distributions of shrinkage strain ϵ_{sh}, which shows how the central portion of the wall begins to develop large shrinkage after many centuries of exposure. Fig. 6h shows the creep data measured by Anzani et al. [3] on specimens of ancient masonry taken from the ruins of Pavia tower; Fig. 6i a three-dimensional model of the wall with cladding, with the assumed failure mode of the wall; and Fig. 6d the calculated size effect as a function of the tower size.

The diffusion and stress redistribution in wall are analyzed by finite differences (e.g. [37,50]) in a manner similar to the analysis of the hydration heat effect in a nuclear containment wall outlined in a preceding section. The nonlinear diffusion equation with a diffusivity strongly dependent on pore humidity h, determined by Bažant and Najjar [20], is used, with the following parameters, same as for a low strength concrete: Diffusivity at saturation $C_1 \approx 0.2$ cm^2/day; humidity at the center of decrease of diffusivity H_c= 0.75, ratio of diffusivity reduction at full drying α_0= 0.05, and exponent in the formula $n = 6$. The initial condition is a constant pore humidity h= 1 for all spatial coordinates x at the time t_0. The boundary conditions are considered as a constant environmental humidity $h = h_e = 0.5$. Owing to the long time scale, the effect of temperature on moisture diffusion is neglected.

In the cladding, moisture can permeate only through the joints. The joints are assumed to have the same permeability and diffusivity as the lime concrete, and the effective diffusivity in the cladding layer is obtained by reducing the diffusivity of lime concrete in proportion to the cross section area fraction of the joints. The three-dimensional perturbation of the flow right beneath the cladding is neglected. Furthermore, the moisture flow from the mortar joints to the bricks, which begins right after mortar-brick contact, and the reverse moisture flow from the bricks to the mortar [43] are neglected (although a more rigorous model oould be introduced [41–43]). For this reason, the humidity within the cladding is assumed as the environmental humidity (Fig. 6e). Moreover, the long-time effects of the shrinkage of the mortar joints may be ignored since it probably gets competed during the first few years after the construction (Fig. 6g).

In addition, the diffusion of carbon dioxide and the carbonation of lime mortar is neglected, along with a possible change of diffusivity due to carbonation [62], which is likely since carbonation usually causes a decrease of porosity [60]. A more rigorous mathematical model would require considering two coupled diffusion processes, namely those or water and of carbon dioxide [53,54]. In the case of the Civic Tower of Pavia, a surface layer of carbonated lime mortar of recent formation was observed [34], but it was very thin, which means that its neglect seems admissible.

Only few measurements of shrinkage of lime mortar are reported in the literature (e.g. [35,57,56]). The ultimate shrinkage of the lime mortar is taken as 0.0003. No data relevant to drying creep (or Pickett effect) and a separation of the effects of cracking and stress-induced shrinkage in the sense of Bažant and Xi [30] seem unavailable, and so a behavior similar to low-strength concrete is simply co-opted.

To calibrate the creep law, we consider the experimental curves measured by Anzani et al. [3] on specimens taken from the ruins of the Tower. In particular, Fig. 6h represents

the variation of vertical strain measured for panels 19-30A and 19-30B in the first period of the tests (1000days), when the load was kept almost constant ($\sigma \cong f'_c$). The same figure shows with a solid line the comparison with the B3 model (assuming $q_1 = 0.000667$/MPa, $q_2 = 0.00045$/MPa, $\lambda_0 = 1$ day, and $m = 0.5$).

Experimental data on small size panels (700 × 500 × 300 mm) are used to calibrate average material properties [4,34]. In particular for lime concrete, we assume Young's modulus $E_c = 1500$ MPa, compressive strength $f'_c = 2.8$ MPa, tensile strength $f_{ct} = f'_c/20$ ([46]), and maximum aggregate size $d_a = 150$ mm. For the cladding, we assume the same strength values but Young's modulus $E_m = 1.5\ E_c$.

Although the symptoms of collapse doubtless develop gradually and should be analyzed together with the time-dependent response, we may be consider, for the sake of simplicity, the entire process of collapse to be sudden, uncoupled from the time-dependent response, starting from the current stress and deformation state obtained in the time-dependent analysis. Because of the scaling of the diffusion within the wall, the symptoms of collapse must appear later in thick walls than in thin ones. The collapse is expected to initially occur in the cladding, whose thickness a is almost independent of the thickness D of the wall. For simple estimation, one may use the approach fom [31] (also [24], assuming the damage zone from which the energy driving failure gets released to be elliptical, with axes a and b (see the dotted zone in Fig. 6), and the crushing of masonry to be characterized by a certain compressive fracture energy G_{fc}. Considering the experimental stress-strain relationships and the measured height of the failed (crushing) zone [4], one may assume $G_{fc} = 1$ N/mm. The energy release from the ellipsoidal zone is

$$\Delta\Pi = a\ b\ c\ \pi\ \sigma^2/6E_m \tag{31}$$

where E_m is the effective elastic modulus, $a = 250$ mm is the thickness of the masonry cladding, $c = kb$ is the height of the elliptical zone and σ is the nominal stress. The height c can be related to length $b$on the basis of the known solution of the stress intensity factor $k(a/D,\ b/D)$ for a quarter-elliptical corner crack in a flat plate (for the complete expressions, see [2]).

If the damage zone propagates within the masonry layer only, a is a constant, and then

$$\partial\Delta\Pi/\partial b = \tfrac{1}{4}G_{fc}\pi a \tag{32}$$

Solving with respect to σ we get

$$\sigma = \frac{\sqrt{6G_{fc}E_m}}{\sqrt{4b(2\,k + b\,k')}} \tag{33}$$

If $b = \beta D$ we obtain the double logarithmic plot in Fig. 6j showing the stress σ as a function of the dimension D of walls, the geometry assumed to be similar ($\delta_c/D =$ constant). The reduction in strength seen (Fig. 6j) indicate the size effect that may reasonably be expected. For small dimensions, the size effect curve is not plotted because different failure modes were seen in experiments [4]. Besides, it is only for the large dimensions that the weight of the tower becomes important [40].

10. CLOSING REMARKS

The theory of creep and shrinkage of concrete has been a rather contentious subject. One cause of the recent heated polemics on the merits of various creep models could be seen in excessive empiricism, or inadequate attention to theoretical and physical arguments. Even though experimental data are at present very plentiful, their bulk is concentrated within only a small portion of the temporal and spatial scales relevant to practice. Since a large random scatter is always present, pure phenomenological or intuitive interpretation of the available data is highly ambiguous. It is simply impossible to figure out or validate the correct creep model by looking at the test data alone.

Among various theoretical and physical aspects, this is where the consideration of temporal and spatial scaling can be of considerable help. To show that, has been the main purpose of this article.

Acknowledgment: Partial financial support from the U.S. National Science Foundation under grant CMS-9713944 is gratefully acknowledged.

REFERENCES

1. Anand, S.C., and Rahman, M.A. (1991). "Numerical modeling of creep in composite masonry walls." *J. Struct. Engrg.*, ASCE, 117(7), 2149–2165.
2. Anderson T.L. (1994) *Fracture Mechanics: Fundamentals and Applications*, 2nd ed., CRC Press, Boca Raton.
3. Anzani, A., Binda, L., and Melchiorri, G. (1995). "Time dependent damage of rubble masonry walls." in *4th International Masonry Conference*, H.W.H. West, ed., British Masonry Society, London, 341–351.
4. Anzani, A., Binda, L., and Mirabella Roberti, G. (2000). "The effect of heavy persistent actions into the behaviour of ancient masonry." *Mat. and Struct.*, RILEM, Paris, 33, 251–261.
5. Barenblatt, G.I. (1979). *Similarity, self-similarity and intermediate asymptotics*, Consultants Bureau, New York, N.Y.
6. Barenblatt, G.I. (1987). *Dimensional analysis*, Gordon and Breach Sci. Publ., New York.
7. Bažant, Z.P. (1982). "Mathematical models for creep and shrinkage of concrete.", in *Creep and Shrinkage of Structures*, Z.P. Bažant and F.H. Wittmann, eds., John Wiley, London, 163–256.
8. Bažant, Z.P. (1997). "Stresses and cracking caused by hydration heat in massive concrete wall." Preliminary Technical Note, submitted to Korea Electric Power Institute, Taejun, Korea.
9. Bažant, Z.P. (1999). "Size effect on structural strength: a review." *Archives of Applied Mechanics* (Ingenieur-Archiv, Springer Verlag), 69, 703–725 (75th Anniversary Issue).
10. Bažant, Z.P. (1999). "Criteria for rational prediction of creep and shrinkage of concrete." *Revue Française de Génie Civil*, 3(3–4), 61–89; also in: *Creep and Shrinkage of Concrete*, ed. by F.-J. Ulm, M. Prat, J.-A. Calgaro and I. Carol, Hermès Science Publications, Paris 1999, 61–89 (reprinted with updates in ACI SP–194, 2000).
11. Bažant, Z.P., and Baweja, S. (1995), in collaboration with RILEM Committee TC

107-GCS, "Creep and shrinkage prediction model for analysis and design of concrete structures—model B3." (RILEM Recommendation), *Mat. and Struct.*, RILEM, Paris, 28, 357–365; with Errata, Vol. 29 (March 1996), p. 126.
12. Bažant, Z.P., and Baweja, S. (1995). "Justification and refinement of Model B3 for concrete creep and shrinkage. 1. Statistics and sensitivity." *Mat. and Struct.*, RILEM, Paris, 28, 415–430.
13. Bažant, Z.P., and Baweja, S. (1995). "Justification and refinement of Model B3 for concrete creep and shrinkage. 2. Updating and theoretical basis." *Mat. and Struct.*, RILEM, Paris, 28, 488–495.
14. Bažant, Z.P., and Baweja, S. (2000). "Creep and shrinkage prediction model for analysis and design of concrete structures: Model B3." *Adam Neville Symposium: Creep and Shrinkage—Structural Design Effects*, ACI SP–194, A. Al-Manaseer, ed., Am. Concrete Institute, Farmington Hills, Michigan, 1–83.
15. Bažant, Z.P., and Cedolin, L. (1991). *Stability of Structures: Elastic, Inelastic, Fracture and Damage Theories*, Oxford University Press, New York.
16. Bažant, Z.P., and Chern, J.-C. (1985). "Strain- softening with creep and exponential algorithm." *J. Engrg. Mech.*, ASCE, 111(3), 391–415.
17. Bažant, Z.P., Hauggaard, A.B., Baweja, S., and Ulm, F.-J. (1997). "Microprestress-solidification theory for concrete creep. I. Aging and drying effects." *J. Engrg. Mech.*, ASCE, 123(11), 1188–1194.
18. Bažant, Z.P., Hauggaard, A.B., and Baweja, S. (1997). "Microprestress-solidification theory for concrete creep. II. Algorithm and verification." *J. Engrg. Mech.*, ASCE, 123(11), 1195–1201.
19. Bažant, Z.P., and Kaplan, M.F. (1996). *Concrete at High Temperatures: Material Properties and Mathematical Models*, Longman (Addison-Wesley), London.
20. Bažant, Z.P., and Najjar, L.J. (1972). "Nonlinear water diffusion in nonsaturated concrete." *Mat. and Struct.*, RILEM, Paris, 5, 3–19.
21. Bažant, Z.P., and Oh, B.-H. (1983). "Crack band theory for fracture of concrete." *Mat. and Struct.*, RILEM, Paris, 16, 155–177.
22. Bažant, Z.P., and Ohtsubo, H. (1977). "Stability conditions for propagation of a system of cracks in a brittle solid." *Mechanics Research Communications*, 4(5), 353–366.
23. Bažant, Z.P., Ohtsubo, R., and Aoh, K. (1979). "Stability and post-critical growth of a system of cooling and shrinkage cracks." *Int. J. of Fracture*, 15, 443–456.
24. Bažant, Z.P., and Planas, J. (1998). *Fracture and Size Effect in Concrete and Other Quasibrittle Materials*, CRC Press, Boca Raton and London.
25. Bažant, Z.P., and Prasannan, S. (1989). "Solidification theory for concrete creep: I. Formulation." *J. Engrg. Mech.*, ASCE, 115(8), 1691–1703.
26. Bažant, Z.P., and Prasannan, S. (1989). "Solidification theory for concrete creep: II. Verification and application." *J. Engrg. Mech.*, ASCE, 115(8), 1704–1725.
27. Bažant, Z.P., and Raftshol, W.J. (1982). "Effect of cracking in drying and shrinkage specimens." *Cement and Concrete Res.*, 12, 209–226; Disc. 797–798.
28. Bažant, Z.P., Şener, S. and Kim, J.-K. (1987). "Effect of cracking on drying permeability and diffusivity of concrete." *ACI Mat. J.*, 84(5), 351–357.
29. Bažant, Z.P., and Steffens, A. (2000). "Mathematical model for kinetics of alkali-silica

reaction in concrete." *Cement and Concrete Res.*, 30(3), 419–428.
30. Bažant, Z.P., and Xi, Y. (1994). "Drying creep of concrete: constitutive model and new experiments separating its mechanisms." *Mat. and Struct.*, RILEM, Paris, 27, 3–14.
31. Bažant, Z.P., and Xiang, Yuyin (1997). "Size effect in compression fracture: splitting crack band propagation." *J. of Engrg. Mechanics* ASCE 123 (2), 162–172.
32. Bažant, Z.P., Zi, G., and Meyer, C. (2000). "Fracture mechanics of ASR in concretes with waste glass particles of different sizes." *J. Engrg. Mech.*, ASCE, 126(3), 226–232.
33. Bender, C.M. and Orszog, S.A. (1978). "Advanced Methematical Methods for Scientists and Engineers." McGraw Hill, New York (Sec. 7.4)
34. Binda, L., Gatti, G., Mangano, G., Poggi, C., and Sacchi Landriani, G. (1992). "The collapse of the Civic Tower of Pavia: a survey of the materials and structure." *Masonry International*, 6, 11–20.
35. Brooks, J.J. (1990). "Composite modelling of masonry deformation." *Mat. and Struct.*, RILEM, Paris, 23, 241–251.
36. Calvi, G.M., and Priestley, M.J.N. (1990). "Post collapse analyses of a medieval masonry tower." in *5th North American Masonry Conference*, D.P. Abrams, ed., Univ. of illinois, Urbana-Champaign, Illinois, 713–722.
37. Crank, J. (1957). *Mathematics of Diffusion*, Oxford University Press, Oxford.
38. Creazza, G., Soranzo, M., Gori, R., Saetta, A., Micali, B., and Bertacchi, L. (1997). "Structural diagnosis of the medieval bell tower in the Town of Aquileia (Italy)." in *5th International Conference on Structural Studies, Repairs and Maintenance of Historical Buildings*, STREMAH97, S. Sanchez-Beitia, C.A. Brebbia, eds., Computational Mechanics Publications, Southampton, UK.
39. Ferretti, D., Iori, I., and Riva, R. (1998). "On the collapse of ancient towers: The failure of the Civic Tower in Pavia (in Italian)." in *Studi e Ricerche*, 19, Politecnico di Milano, Milan, 169–191.
40. Ferretti, D., Iori, I., and Rizzi, G. (2000). "The role of size effect in compression failure of ancient towers." in *More than Two Thousand Years in the History of Architecture*, G. Croci, ed., ICOMOS-UNESCO, Bethlem, Ib 15.
41. Forth, J.P., Brooks, J.J. (1995). "Influence of mortar type on long term deformation of single leaf clay brick masonry." in *4th International Masonry Conference*, H.W.H. West, ed., British Masonry Society, London, 157–161.
42. Forth, J.P., Brooks, J.J., and Tapsir, S.H. (2000). "The effect of unit water absorption on long term movements of masonry." *Cement and Concrete Composites*, 22, 273–280.
43. Groot, C., and Larbi, J. (1999). "The influence of water flow (reversal) on bond strength development in young masonry." *Heron*, Delft, 44(2), 63–78.
44. Heinle, E., and Leonhardt, F. (1989) *Towers: A Historical Survey*, Rizzoli, New York.
45. Heyman, J. (1992). "Leaning towers." *Meccanica*, 27, 153–159.
46. Jamiolkowski, M., Lancellotta, R. and Pepe, C. (1993). "Leaning Tower of Pisa – Updated information." in *3rd International Conference on Case Histories in Geotechnical Engineering*, University of Missouri-Rolla, Rolla MO, 1–12.
47. Lenczer, D. (1986). "In-situ measurement of creep movement in a brick masonry tower block." *Masonry International*, 8, 17–20.
48. Leonhardt, F. (1998). "Saving the Tower of Pisa – a report." *Indian Concr. J.*, 72(5),

247–250.
49. Mangui, M., and Ulm, F.-J. (2000). *Coupled Diffusion-Dissolution Around a Fracture.* Report, Department of Civil Engineering, M.I.T.
50. Özisik, N.M. (1994). *Finite difference methods in heat transfer*, CRC Press, Boca Raton.
51. Planas, J., Elices, M. (1993). "Drying shrinkage effects on the modulus of rupture." in *5th Int. RILEM Symp., Barcelona*, Z.P. Bažant and I. Carol, eds., E & FN Spon, London, 357–368.
52. RILEM Committee TC 69 (1988) (Z.P. Bažant, Chairman), "State of the art in mathematical modeling of creep and shrinkage of concrete." in *Mathematical Modeling of Creep and Shrinkage of Concrete*, Z.P. Bažant, ed., J. Wiley, Chichester and New York, 57–215.
53. Saetta, A.V., Schrefler, B.A., and Vitaliani, R. (1993). "The carbonation of concrete and the mechanism of moisture, heat and carbon dioxide flow through porous materials." *Cement and Concrete Res.*, 23, 761–772.
54. Saetta, A.V., Schrefler, B.A., and Vitaliani, R. (1995). "2-D model for moisture for carbonation and moisture/heat flow in porous materials." *Cement and Concrete Res.*, 25, 1703–1712.
55. Sedov, L.I. (1959). *Similarity and dimensional methods in mechanics*, Academic Press, New York.
56. Shrive, N.G., Sayed-Ahmed, E., and Tilleman, D. (1997). "Creep analysis of clay masonry assemblages." *Can. J. of Civ. Eng.*, 24, 367–379.
57. Sickels Taves, L.B. (1995). "Creep, Shrinkage, and Mortars in Historic Preservation." *J. of Testing and Evaluation*, 23, 447–452.
58. Ulm, F.-J. (1999). *Revue Française de Génie Civil*, 3, 3–4.
59. Ulm, F.-J. (1999). "Chemoporoplasticity of calcium leaching in concrete." *J. Engrg. Mech.*, ASCE, 125(10), 1200–1211.
60. van Balen, K., and van Gemert, D. (1994). "Modelling lime mortar carbonation." *Mat. and Struct.*, RILEM, Paris, 27, 393–398.
61. Wittmann, F.H. (1982). "Creep and shrinkage mechanisms." in *Creep and shrinkage of concrete structures*, Z.P. Bažant and F.H. Wittmann, eds., J. Wiley, London 129–161.
62. Ying-yu, L., and Qui-dong, W. (1989). "The mechanism of carbonation of mortars and the dependence of carbonation on pore structure", in *Concrete Durability*, J.M Scanlon, ed., ACI SP-100, Am. Concrete Inst., Detroit, 1915–1929.